A STUDY ON RESPONSE ANALYSIS OF MACHINE STRUCTURE SYSTEM SUBJECTED TO TWO SEISMIC MOTIONS

by Hisayoshi SATO and Kohei SUZUKI

1. Introduction

Generally piping system and other machine structure system as crane and boiler attached to building or ground are subjected to more than one seismic motions directly or indirectly. In this paper attention is focussed on this fact and the dynamic response characteristics of such structure system, are investigated. It is necessary for us to obtain wave forms not only of acceleration but of velocity and displacement in order to make the analysis. So some discussions are done about a method to obtain velocity and displacement wave form from the record of ground acceleration by making use of analog computer. [1) 2)]

By using thus obtained wave forms of acceleration, velocity and displacement, response of the system directly subject to two seismic motions with certain time-lag interval is computed by analog computer. And a statistical approach for this system is briefly investigated. Finally the response spectra of a building-machine structure system composed by aforementioned system are given.

2. Basic Equations [3)]

At first simple mass-spring systems are considered which are shown in Fig. 1. These are the simplest one subjected to multi-seismic motions. The dynamic behaviour of such structures as piping, transporter, crane, bridge and so on could be simulated fundamentally by these models.

The equation of motion for I in Fig. 1 is given as

$$m\ddot{X}+c_1(\dot{X}-\dot{Y}_1)+k_1(X-Y_1)-c_2(\dot{X}-\dot{Y}_2)-k_2(X-Y_2)=0 \tag{1}$$

and for II

$$\begin{aligned} &m_1\ddot{X}_1+c_1(\dot{X}_1-\dot{Y}_1)+k_1(X_1-Y_1)-c_2(\dot{X}_2-\dot{X}_1)-k_2(X_2-X_1)=0 \\ &m_2\ddot{X}_2+c_2(\dot{X}_2-\dot{X}_1)+k_2(X_2-X_1)-c_3(\dot{Y}_2-\dot{X}_2)-k_3(Y_2-X_2)=0 \end{aligned} \tag{2}$$

where X, X_1, X_2, Y_1 and Y_2 are the absolute displacement, m, m_1 and m_2 are the mass, c, c_1, c_2 and c_3 are the damping coefficient, k, k_1, k_2 and k_3 are the stiffness. Assuming that damping and stiffness are qual for simplicity, (1) and (2) can be transformed to the equations in terms of relative displacement for each boundary, [4)]

$$(\ddot{X}-\ddot{Y}_1)+2h_s\omega_s(\dot{X}-\dot{Y}_1)+\omega_s^2(X-Y_1)=-\ddot{Y}_1+h_s\omega_s(\dot{Y}_2-\dot{Y}_1)+\frac{\omega_s^2}{2}(Y_2-Y_1)$$
$$(\ddot{X}-\ddot{Y}_2)+2h_s\omega_s(\dot{X}-\dot{Y}_2)+\omega_s^2(X-Y_2)=-\ddot{Y}_2-h_s\omega_s(\dot{Y}_2-\dot{Y}_1)-\frac{\omega_s^2}{2}(Y_2-Y_1) \quad (3)$$

$$(\ddot{X}_1-\ddot{Y}_1)+4h_s\omega_s(\dot{X}_1-\dot{Y}_1)+2\omega_s^2(X_1-Y_1)-2h_s\omega_s(\dot{X}_2-\dot{Y}_1)-\omega_s^2(X_2-Y_1)=-\ddot{Y}_1$$
$$(\ddot{X}_2-\ddot{Y}_1)+4h_s\omega_s(\dot{X}_2-\dot{Y}_1)+2\omega_s^2(X_2-Y_1)-2h_s\omega_s(\dot{X}_1-\dot{Y}_1)-\omega_s^2(X_1-Y_1)$$
$$=-\ddot{Y}_1+2h_s\omega_s(\dot{Y}_2-\dot{Y}_1)+\omega_s^2(Y_2-Y_1)$$
$$(\ddot{X}_1-\ddot{Y}_2)+4h_s\omega_s(\dot{X}_1-\dot{Y}_2)+2\omega_s^2(X_1-Y_2)-2h_s\omega_s(\dot{X}_2-\dot{Y}_2)-\omega_s^2(X_2-Y_2) \quad (4)$$
$$=-\ddot{Y}_2-2h_s\omega_s(\dot{Y}_2-\dot{Y}_1)-\omega_s^2(Y_2-Y_1)$$
$$(\ddot{X}_2-\ddot{Y}_2)+4h_s\omega_s(\dot{X}_2-\dot{Y}_2)+2\omega_s^2(X_2-Y_2)-2h_s\omega_s(\dot{X}_1-\dot{Y}_2)-\omega_s^2(X_1-Y_2)=-\ddot{Y}_2$$

where $h_s=\frac{c}{2\sqrt{mk}}$, $\omega_s^2=\frac{k}{m}$

These equations are very useful for dynamic analysis by analog computation especially for the case that the analysis of the system combining machine structure with building structure system is objective.

3. Integral of Ground Acceleration [5]

Equations (3) and (4) have not only terms of the acceleration at boundaries but also the terms which are based on relative velocity $(\dot{Y}_1-\dot{Y}_2)$ and relative displacement (Y_1-Y_2) as external force. If $\ddot{Y}_1$ and $\ddot{Y}_2$ are considered to be ground acceleration, it is necessary to obtain ground velocity and displacement. So first of all, a method to obtain wave forms of velocity and displacement by integrating that of acceleration through analog computer is investigated. The difficulty that integrated wave form easily diverses in case of direct integral is prevented by a proposed approximate integral. Fig. 2 shows block diagram of the approximate integral operation by analog computer. The characteristic of the approximate integral is same as that of one-degree-of-freedom system, the natural period of which is taken longer than band width of the earthquake record. (dotted line in Fig. 2). If the acceleration wave form is added to the system, the integral is carried out for the components of the earthquake, however at the same time transient response of the system with long natural period T_0 is excited. T_0 can be chosen as various values considering frequency components of each earthquake record. For the earthquake containing long period the larger T_0 has to be chosen. In order to suppress the divergency of the wave, at first certain amount of damping (damping ratio h) is introduced to the approximate integral system. Next to get rid of these long period component, the integrated wave form go through high pass filter shown as within solid line in Fig. 2. An ap-

propriate break period T_s has to be chosen by taking the bandwidth of earthquake motion, the natural period and the damping ratio of the integral system into consideration.

The transfer function for this proposed integral system is written as

$$G(s) = G_1(s) \cdot G_2(s) = \frac{s}{s^2 + 2hws + w_0^2} \cdot \frac{Ts\ s}{1 + Ts\ \ s} \tag{5}$$

where $G_1(s)$ is the transfer function for the integral system and $G_2(s)$ is that of the high-pass filter. In Fig. 3 - Fig. 8 some examples of the gain-phase characteristics of this operation used in their practice are shown. Δg (dB) is the gain error from the theoretical integral and θ shows phase characteristics. It might be recommended that for Δg and θ less than about 0.25 dB and 10° these operations keep the gain and phase characteristics of the integral.

Then this proposed integral method is applied to some actual earthquake wave forms. For example let us pick up those of El Centro (NS, May, 1940) and Niigata (NS, June, 1964) earthquakes. [6] The former is the well-known typical earthquake and the latter is the one in which long period component is predominant. To look over the characteristics of these earthquakes, the response spectrum of one-mass-system are shown in Fig. 9 through Fig. 14. Considering these results, T_0 = 8.0 sec, T_s = 5.0 sec and h = 0.1 for El Centro, T_0= 20.0 sec, T_s = 10.0 sec and h = 0.1 are chosen. In Fig. 15 and Fig. 16 acceleration and the computed wave forms of velocity and displacement are shown for both earthquakes. If maximum acceleration are taken 0.30 g for El Centro and 0.16 g for Niigata due to actual data, computed velocity and displacement are 57.0 cm/sec, 12.7 cm and 48.0 cm/sec, 42.0 cm respectively. In Tab. 1 several examples of thus obtained maximum value of velocity and displacement are shown.

4. Response of the System Subjected to Two Inputs with Certain Time-Lag Interval [7]

As a simple example the response of the one-degree-of freedom system due to two earthquake motions, which have same wave form but one of which lags behind the other with a certain interval, is investigated. When T_ℓ represents this time-lag interval,

$$Y_2(t) = Y_1(t+T_\ell),\quad \dot{Y}_2(t) = \dot{Y}_1(t+T_\ell),\quad \ddot{Y}_2(t) = \ddot{Y}_1(t+T_\ell) \tag{6}$$

are given in eq. (3).

This is the simplest idealisation for actual system considering wave propagation. Some response characteristics of the system to earthquake motions are made obvious. Block diagram of this computation is shown in Fig. 17. Solid line in Fig. 18 is the normalized acceleration response of the model for El Centro by taking T_ℓ as the abscissa.

Next a brief statistical investigation is described for this system with the assumption that earthquake motion is a stationary random process.[8] If the following Z is introduced,

$$Z = X - \frac{1}{2}(Y_1 + Y_2) \tag{7}$$

so eqs. (3) can be written as

$$\ddot{Z} + 4 h_s \omega_s \dot{Z} + 2\omega_s^2 Z = -\frac{1}{2}(\ddot{Y}_1 + \ddot{Y}_2) \tag{8}$$

Equation (8) can be written by using the Laplace transform operator,

$$\left(\frac{s^2 + 4 h_s \omega_s s + 2\omega_s^2}{s^2}\right) Z(s) = \frac{1}{2}\{G_1(s) + G_2(s)\} \tag{9}$$

where $Z(s)$, $G_1(s)$ and $G_2(s)$ are the Laplace transform of Z, $\ddot{Y}_1$ and $\ddot{Y}_2$ respectively. When $X(s)$ represents the transform of X from eq. (7)

$$Z(s) = X(s) - \frac{1}{2}\{G_1(s) + G_2(s)\} \tag{10}$$

Then, as for X the following equation is given

$$X(s) = \frac{1}{2} \cdot \frac{2 h_s \omega_s s + \omega_s^2}{s^2 + 2 h_s \omega_s s + \omega_s^2}\{G_1(s) + G_2(s)\} \tag{11}$$

This equation can be applied to the one-degree-of-freedom system subjjected to two random inputs. When relations (6) are considered,

$$G_2(s) = e^{Ts} \cdot G_1(s) \tag{12}$$

Therefore, as the results the ratio of the acceleration response to the ground, denoted by λ_a can be written by the following expression.

$$\lambda_a^2 = \frac{1}{2} \frac{\int_0^\infty h_1(s)\, ds + 2\int_0^\infty h_2(s)\, ds}{\int_0^\infty g(s)\, ds} \tag{13}$$

where from Kanai's formula the transfer function of the ground model

$$g(s) = \left| \frac{2 h_g \omega_g s + \omega_g^2}{s^2 + 2 h_g \omega_g s + \omega_g^2} \right|^2 \tag{14}$$

and

$$h_1(s) = \left| \frac{2h_g w_g s + w_g^2}{s^2 + 2h_g w_g s + w_g^2} \cdot \frac{2h_s w_s s + w_s^2}{s^2 + 2h_s w_s s + w_s^2} \right|^2 \tag{15}$$

$$h_2(s) = \left(e^{Ts} + e^{-Ts} \right) \cdot h_1(s) \tag{16}$$

Using $s = j\omega$, eq. (13) can be written as

$$\lambda a^2 = \frac{1}{2} \frac{\int_0^\infty h_1(\omega)\, d\omega + \int_0^\infty h_1(\omega) \cos T\ell\omega \; d\omega}{\int_0^\infty g(\omega)\, d\omega} \tag{17}$$

Dotted line in Fig. 18 shows the diagram of an acceleration response curve taking $T\ell$ as the abscissa through the computation of eq. (17). Two lines depict pretty good concidence. These graphs show wavy shape which has maximum values at $T\ell = (n-1)Ts$ and minimum values at $T\ell = (n - \frac{1}{2})Ts$ $(n = 1, 2, \ldots\ldots)$.

The response at $T\ell = 0$ takes the maximum for any case. In similar way displacement response can be computed. Fig. 19 shows the relative displacement response by an earthquake record through analog computer. Fig. 20 is an example of the theoretical results from the statistical computation. These response curves also show similar characteristics. It should be pointed out that displacement response might have a serious effect on the structure system.

5. Simple Example of The Building-Machine Structure System and Its Response Spectra [9]

Now consider the whole building-machine structure system as shown in Fig. 21. For simplicity let us make $m_1 = m_2 = m$, $k_1 = k_2 = k_3 = k$, $c_1 = c_2 = c_3 = c$ and $M_1 = M_2 = M$. Assuming the first mode shape of motion for the building system as in Fig. 22, the relation $K_2/K_1 = 2/3$ and $C_2/C_1 = \sqrt{2/3}$ are given. [10] The equations for the motion for the whole system can be written as

$$\left\{ \begin{aligned} &(\ddot{Y}_1 - \ddot{Y}) + \left(\frac{C_1}{M} + \frac{C_2}{M}\right)(\dot{Y}_1 - \dot{Y}) + \left(\frac{K_1}{M} + \frac{K_2}{M}\right)(Y_1 - Y) - \frac{C_2}{M}(\dot{Y}_2 - \dot{Y}) - \frac{K_2}{M}(Y_2 - Y) \\ &\qquad = -\ddot{Y} + \frac{rc}{m}(\dot{X}_1 - \dot{Y}_1) + \frac{rk}{m}(X_1 - Y_1) \end{aligned} \right. \tag{18}$$

$$\left\{ \begin{aligned} &(\ddot{Y}_2 - \ddot{Y}) + \frac{C_2}{M}(\dot{Y}_2 - \dot{Y}) + \frac{K_2}{M}(Y_2 - Y) - \frac{C_2}{M}(\dot{Y}_1 - \dot{Y}) - \frac{K_2}{M}(Y_1 - Y) \\ &\qquad = -\ddot{Y} + \frac{rc}{m}(\dot{X}_2 - \dot{Y}_2) + \frac{rk}{m}(X_2 - Y_2) \end{aligned} \right. \tag{19}$$

$$(\ddot{X}_1-\ddot{Y}_1)+\frac{2c}{m}(\dot{X}_1-\dot{Y}_1)+\frac{2k}{m}(X_1-Y_1)-\frac{c}{m}(\dot{X}_2-\dot{Y}_1)-\frac{k}{m}(X_2-Y_1)=-\ddot{Y}_1 \quad (20)$$

$$(\ddot{X}_2-\ddot{Y}_1)+\frac{2c}{m}(\dot{X}_2-\dot{Y}_1)+\frac{2k}{m}(X_2-Y_1)-\frac{c}{m}(\dot{X}_1-\dot{Y}_2)-\frac{k}{m}(X_1-Y_2) =-\ddot{Y}_1+\frac{c}{m}(\dot{Y}_2-\dot{Y}_1)+\frac{R}{m}(Y_2-Y_1) \quad (21)$$

$$(\ddot{X}_1-\ddot{Y}_2)+\frac{2c}{m}(\dot{X}_1-\dot{Y}_2)+\frac{2k}{m}(X_1-Y_2)-\frac{c}{m}(\dot{X}_2-\dot{Y}_2)-\frac{k}{m}(X_2-Y_2) =-\ddot{Y}_2+\frac{c}{m}(\dot{Y}_1-\dot{Y}_2)+\frac{k}{m}(Y_1-Y_2) \quad (22)$$

$$(\ddot{X}_2-\ddot{Y}_2)+\frac{2c}{m}(\dot{X}_2-\dot{Y}_2)+\frac{2k}{m}(X_2-Y_2)-\frac{c}{m}(\dot{X}_1-\dot{Y}_2)-\frac{k}{m}(X_1-Y_2)=-\ddot{Y}_2 \quad (23)$$

Eqs. (18) and (19) are as for the building system, from eq. (20) to eq. (23) are as for the machine structure system. Both systems are connected with each other by only boundary conditions which are the second and third terms of the right hand side in eqs. (18) and (19) and those in eqs. (21) and (22). $\gamma=m/M$ means mass ratio of the machine structure to the building.

$\gamma=0$ means that the building structure receives no force reaction from the machine structure. When $\gamma\neq 0$, reactions $\gamma(c/m)(\dot{X}-\dot{Y})$ and $\gamma(k/m)(X-Y)$ exist. In Fig. 23, block diagram for this analysis is shown. These equations are transformed into those of the normal coordinate. This normalized form is effective to observe the first or second mode of motion separately.

The response characteristics are investigated for this system by analog computer. As the records, El Centro and Taft (NS, July, 1952) are used.

Fig. 24 shows an example of the displacement spectra and Fig. 25 does that of the acceleration spectra, where the natural period of the machine system T_m is taken as the abscissa, that of building structure for the first mode T_b as the parameter. As shown in Fig. 25, the ratio of the maximum acceleration of the response to the maximum ground acceleration $\frac{\alpha_m}{\alpha_g}$ shows a sharp peak at every $T_b=T_m$. This tendency is conspicuous especially in shorter period as T_b = 0.2, 0.4, 0.6 sec. As for the relative displacement, $T_b=T_m$ also makes peak in the spectrum. However, the peak value is greater in longer period as in Fig. 24. These results show that the coincidence of both structure periods ($T_b=T_m$) should be evaded from the viewpoint of the aseismic design of machine structure.

In Fig. 26 the response of acceleration combining the worst conditions $T_b = T_m$ is shown. Let us call this graph "$T_b - T_m$ response spectrum". h_m is selected as parameter. Fig. 27 shows an example of the relation α_m and h_m, where γ (mass ratio) is taken as parameter. The response spectrum decreases as the mass ratio becomes large.

6. Conclusions

(1) The equations of motion for the structure subjected to two inputs can be analyzed by making terms based on the relative displacement and velocity as exciting forces.

(2) Earthquake velocity and displacement wave forms can be easily and stably obtained from acceleration through the approximate integral by analog computer.

(3) Response curves of the system subjected to two seismic motions with certain time-lag interval T_ℓ show wavy shape in relation to T_ℓ. The tendency fairly well coincides with that by the statistical analysis.

(4) In response spectrum of whole building-machine structure system, coincidence of both structures is the worst condition from the viewpoint of aseismic design of annexed machine structure likewise in the case of single input.

(5) An h_m and γ becomes larger, the value of response becomes smaller.

7. Acknowledgements

In closing the authors would like to express their thanks to Professors F. Fujii, A. Watari and H. Shibata at University of Tokyo for their constructive discussions and special thanks go to Professor Emeritus H. Kawasumi and Professor Y. Sato of Earthquake Research Institute at University of Tokyo for their helpul suggestions. They also owe much to Professor H. Umemura who kindly allowed to use earthquake records for SERAC. One of the authors is grateful to Mr. N. Shimizu for his discussions.

8. References

1) H. Sato: On the Response Spectrum of the Machine Structure System to the Strong Motion Earthquake. Bull. JSME 9-36, (1966-11)
2) K. Nakagawa et al.: Preliminary Study on Modal Analysis of Response of a Structure Subjected to Two Different Earthquake Motion at Its Two Supporting Points. Int. Inst. Seism. and Earthq. Engg. (1967-8)
3) H. Sato and K. Suzuki: Response of Building-Machine Structure System Subjected to Two Seismic Motions, Jour. I.I.S., 20-9, (1968-9)
4) S. Okamoto and Y. Hayashi: Response of a Structure to Two inputs, Jour. I.I.S., 21-3, (1969-3)
5) K. Suzuki and H. Sato: On a Method to Obtain Displacement Wave Form from the Record of Earthquake Acceleration, Jour. I.I.S., 22-1, (1970-1)
6) SERAC: Nonlinear Response Analysis of Tall Building to Strong Earthquake and its Application to Aseismic Design, No. 6, (1966-10)
7) H. Sato and K. Suzuki: Response of Structure Subjected to Two Seismic Motions with Certain Time-Lag Interval, Jour. I.I.S., 21-3, (1969-3)
8) H. Tajimi: Basic Theories on Aseismic Design of Structure, Rep. of the Inst. of Ind. Sci., Univ. of Tokyo, 8-4, (1959-3)
9) G. W. Housner et al.: Spectrum Analysis of Strong Motion Earthquakes, Bull. Seim. Soc. Am. 43-2, (1953-4)
10) J. Penzien and A.K. Chopra: Proceed. III-WCEE II/11 (1965-2)

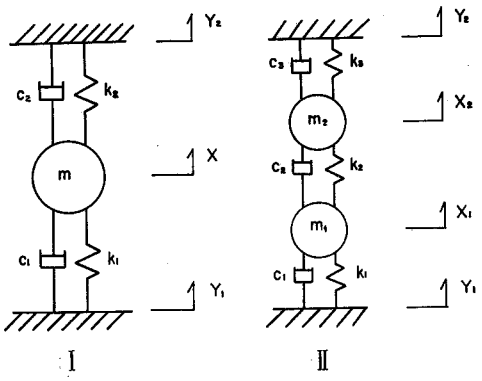

Fig. 1 Simple models of structure

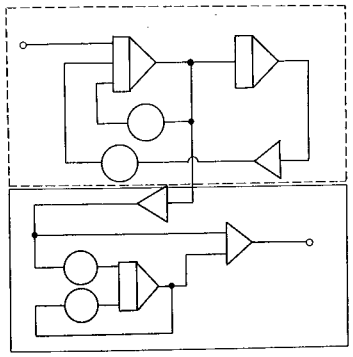

Fig. 2 Block diagram for integral by analog computer

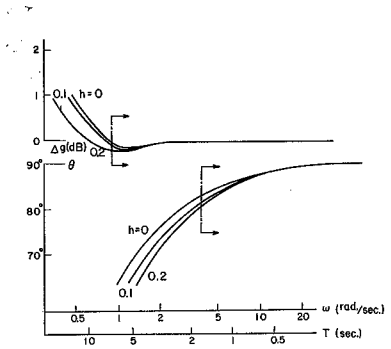

Fig. 3 Gain-phase characteristics of the transfer function G(s) (1). T_s = 2.0 sec, ω_0 = 0.3 rad/sec.

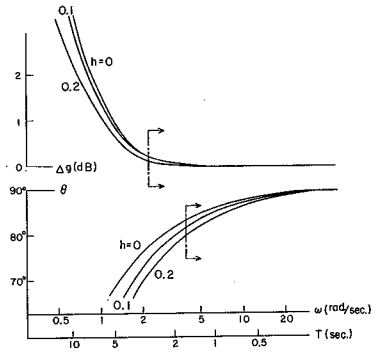

Fig. 4 Gain-phase characteristics of the transfer function G(s) (2). T_s = 2.0 sec, ω_0 = 0.5 rad/sec.

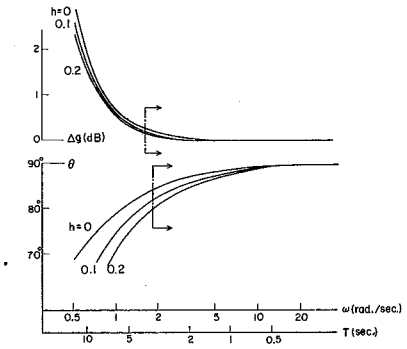

Fig. 5 Gain-phase characteristics of the transfer function G(s) (3). T_s = 5.0 sec, ω_0 = 0.3 rad/sec.

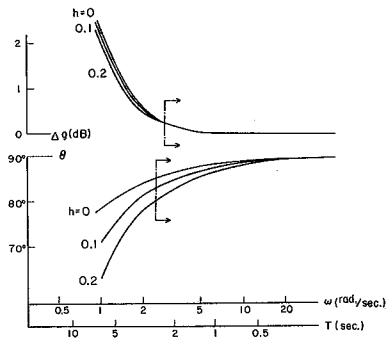

Fig. 6 Gain-phase characteristics of the transfer function G(s) (4). T_s = 5.0 sec, ω_0 = 0.5 rad/sec.

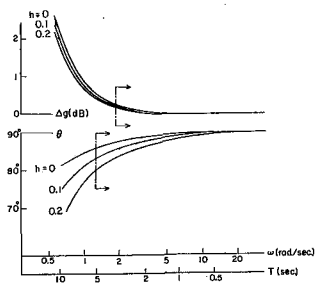

Fig. 7 Gain-phase characteristics of the transfer function G(s) (5). T_s = 10.0 sec, ω_o = 0.3 rad/sec.

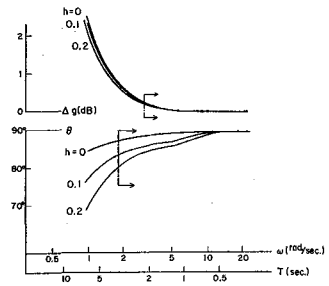

Fig. 8 Gain-phase characteristics of the transfer function G(s) (6). T_s = 10.0 sec, ω_o = 0.5 rad/sec.

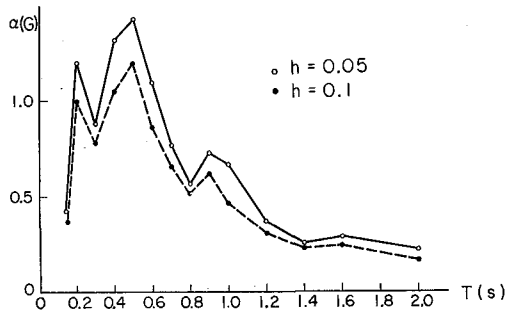

Fig. 9 Acceleration response spectrum for El Centro

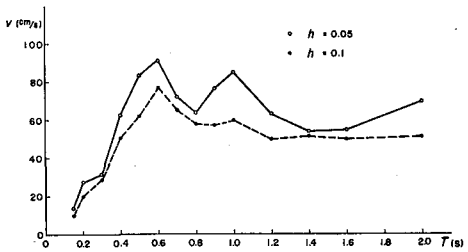

Fig. 10 Velocity response spectrum for El Centro

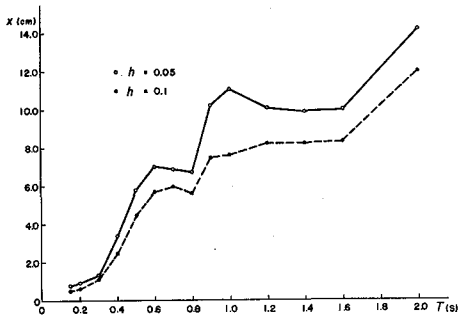

Fig. 11 Displacement response spectrum for El Centro

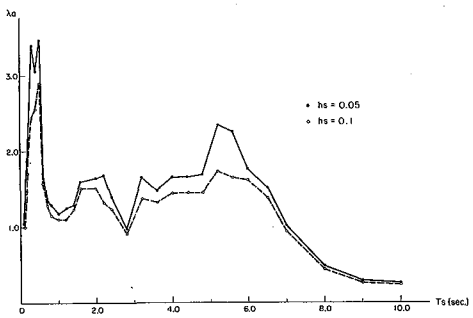

Fig. 12 Acceleration response spectrum for Niigata

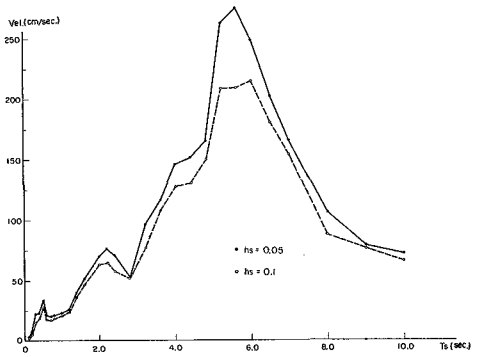

Fig. 13 Velocity response spectrum for Niigata

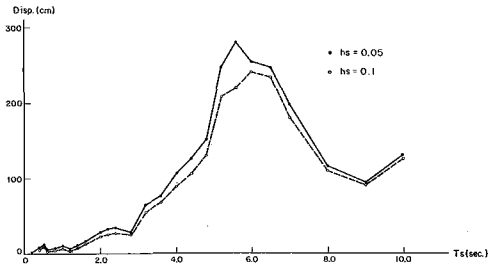

Fig. 14 Displacement response spectrum for Niigata

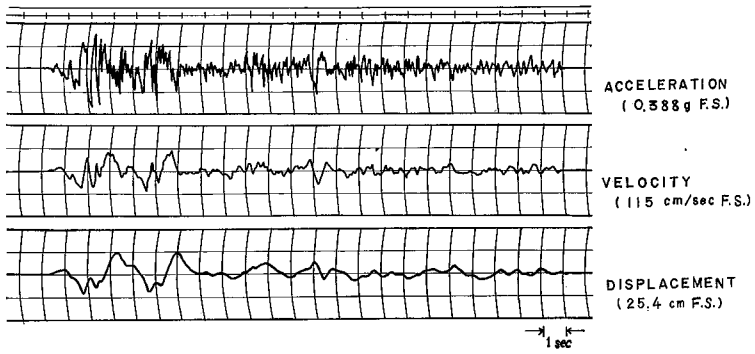

Fig. 15 Earthquake record and its integrated velocity and displacement for El Centro

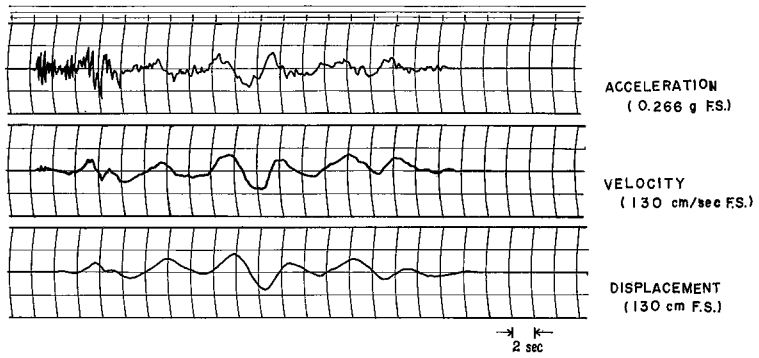

Fig. 16 Earthquake record and its integrated velocity and displacement for Niigata

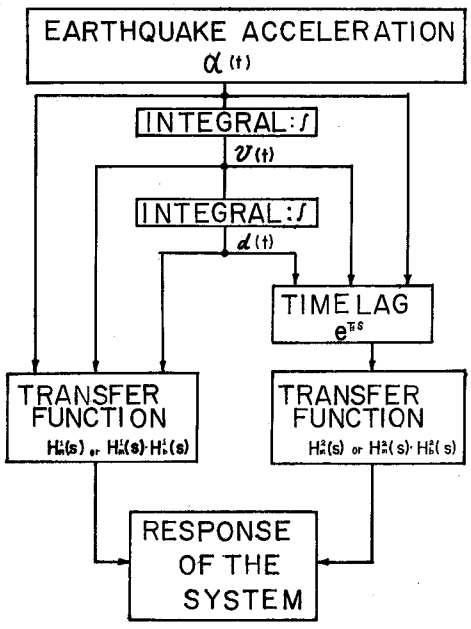

Fig. 17 Block diagram for computation

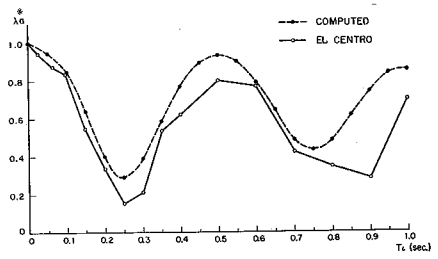

Fig. 18 Acceleration response as abscissa T_ℓ

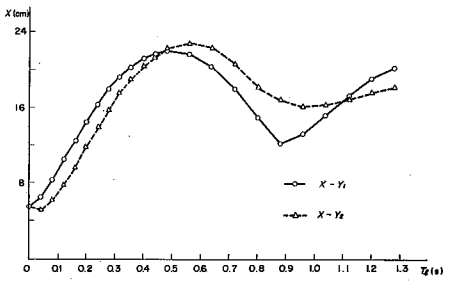

Fig. 19 Displacement response as abscissa T_ℓ

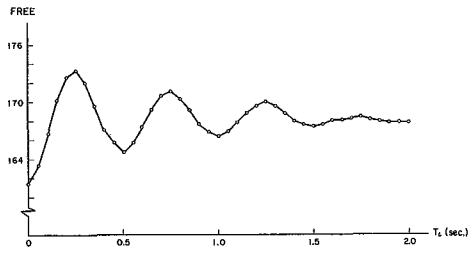

Fig. 20 Theoretical displacement response curve as abscissa T_ℓ ($T = 0.5$ sec, $h = 0.1$)

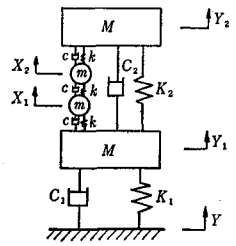

Fig. 21 A model of the building-machine structure system

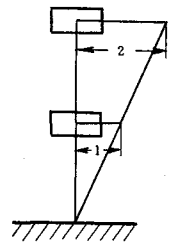

Fig. 22 Mode shape for building system

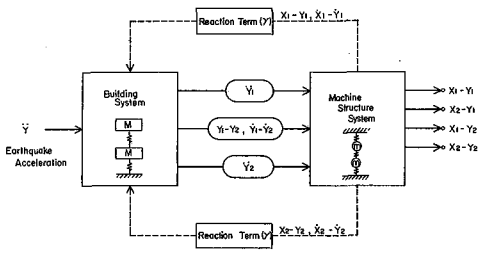

Fig. 23 Block diagram for response analysis by analog computer

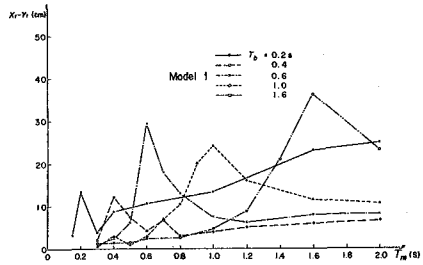

Fig. 24 Displacement response for Taft ($h_b = 0.05$, $h_m = 0.02$, $\gamma = 0$)

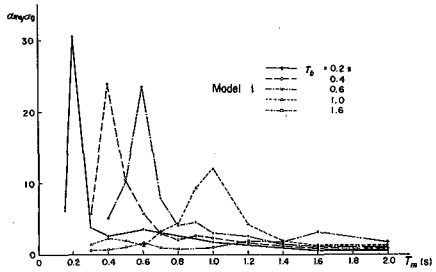

Fig. 25 Acceleration response for El Centro ($h_b = 0.05$, $h_m = 0.02$, $\gamma = 0$)

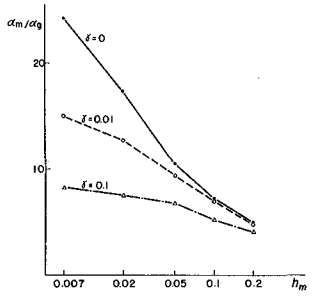

Fig. 26 Relation between α_m/α_g and h_m

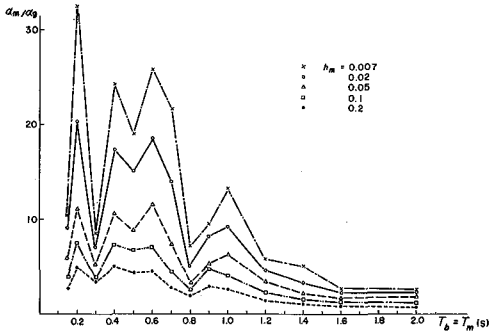

Fig. 27 T_b-T_m acceleration response spectrum for El Centro ($\gamma = 0.01$, $h_b = 0.05$)

Tab. 1 Computed maximum velocity and displacement for various earthquakes

	Max. Vel. (kine)	Max. Disp. (cm)
Akita NS (Jun. 1964)	70.0	14.0
Niigata NS (Jun. 1964)	90.0	78.0
Kushiro NS (Dec. 1961)	21.0	3.5
	18.3 EW	4.2
Oita-oki NS	49.0	11.7
Saitama NS (Feb. 1956)	32.2	6.3
Echizen-oki NS	63.0	17.7
Shizuoka EW (Apr. 1965)	39.0	9.7
Matsushiro EW	33.5	8.1
Taft NS (Jul. 1952)	48.8	10.9
El Centro NS (May 1940)	57.0	12.7

Maximum Acceleration; 0.30 g